

## Grazing mortality as a controlling factor in the uncultured non-cyanobacterial diazotroph (Gamma A) around the Kuroshio region

Takuya Sato<sup>1, a</sup>, Tamaha Yamaguchi<sup>2</sup>, Kiyotaka Hidaka<sup>2</sup>, Sayaka Sogawa<sup>2</sup>, Takashi Setou<sup>2</sup>, Taketoshi Kodama<sup>2, b</sup>, Takuhei Shiozaki<sup>3</sup>, and Kazutaka Takahashi<sup>1</sup>

<sup>1</sup> Graduate School of Agricultural and Life Sciences, The University of Tokyo, Tokyo, 113-8657, Japan

<sup>2</sup> Fisheries Resources Institute, Japan Fisheries Research and Education Agency, Kanagawa, 236-8648, Japan

<sup>3</sup> Atmosphere and Ocean Research Institute, The University of Tokyo, Chiba, 277-8564, Japan

<sup>a</sup> Present address: Institute for Chemical Research, Kyoto University, Kyoto, 611-0011, Japan

10 <sup>b</sup> Present address: Graduate School of Agricultural and Life Sciences, The University of Tokyo, Tokyo, 113-8657, Japan

Correspondence to: Takuya Sato (takusato@scl.kyoto-u.ac.jp)

15 **Abstract.** Nitrogen-fixing microorganisms (diazotrophs) significantly influence marine productivity by reducing nitrogen gas into bioavailable nitrogen. Recently, non-cyanobacterial diazotrophs (NCDs) have been identified as important contributors to marine nitrogen fixation. Among them, Gamma A is one of the best-studied marine NCDs because of its ubiquitous occurrence; however, the factors controlling its distribution remain unknown. In particular, the importance of microzooplankton grazing as a top-down control has not yet been examined. In this study, we investigated the diazotroph community structure using *nifH* amplicon sequencing and quantified the growth and microzooplankton grazing mortality rate of Gamma A using a combination of dilution experiments and quantitative PCR in well-lit waters at the northern edge of the Kuroshio Current off the southern coast of Japan. In the study region, Gamma A was ubiquitous and dominant in the diazotroph communities, whereas cyanobacterial diazotrophs had lower relative abundances. The microzooplankton grazing rate of Gamma A was significantly higher than that of the whole phytoplankton community and was generally balanced with its growth rate, suggesting efficient transfer of fixed nitrogen by Gamma A to higher trophic levels. Although the growth rates of Gamma A did not show clear responses to nutrient amendments, Gamma A abundance had a significant relationship with nutrient concentration and microzooplankton grazing mortality rate. This suggests that microzooplankton grazing, as well as nutrient concentration, plays a vital role in constraining Gamma A distribution in the Kuroshio region. Our findings highlight the importance of further in situ quantification of microzooplankton grazing rates to understand the distribution of diazotrophs and its associated nitrogen transfer into the food web.

20  
25  
30

削除: in situ

削除: negative

削除: microzooplankton grazing

削除: rather than

削除: ,

## 1 Introduction

Biological nitrogen fixation converts inert nitrogen gas into bioavailable nitrogen in the form of ammonia, influencing primary production, and consequently, carbon sequestration through biological pumps in marine ecosystems (Gruber and Galloway, 2008; Karl et al., 1997). Biological nitrogen fixation is performed by specialised prokaryotes called diazotrophs. These include cyanobacterial and non-cyanobacterial groups, which are commonly detected and quantified using the amplified *nifH* gene, which encodes a subunit of the nitrogenase enzyme (Zehr and Capone, 2021). Cyanobacterial diazotrophs such as *Trichodesmium* and *Crocospaera* have long been recognised as important marine diazotrophs (Luo et al., 2012; Zehr, 2011; Shao et al., 2023), whereas non-cyanobacterial diazotrophs (NCDs) were also widely detected in the ocean (Bombar et al., 2016; Farnelid et al., 2011; Turk-Kubo et al., 2023) and dominant in *nifH* gene pools in some regions such as the Arctic Ocean (Blais et al., 2012; Shiozaki et al., 2018b), Indian Ocean (Sato et al., 2022; Shiozaki et al., 2014a), South China Sea (Ding et al., 2021), and South Pacific Ocean (Halm et al., 2012; Moisander et al., 2014). Recently, PCR-free metagenomic and metatranscriptomic studies also revealed the presence and activity of NCDs belonging to diverse phyla such as *Bacteroidota*, *Campylobacterota*, *Myxococcota*, *Planctomycetes*, and *Proteobacteria* in the global ocean (Salazar et al., 2019; Delmont et al., 2022; Delmont et al., 2018; Shiozaki et al., 2023).

Among NCDs, Gamma A, also referred to as AO15 (Zehr et al., 1998), UMB (Bird et al., 2005), and  $\gamma$ -24774A11 (Moisander et al., 2008), is the best-studied marine NCD. Although a recent study identified Gamma A as belonging to the class  $\alpha$ -proteobacteria and potentially having a symbiotic lifestyle (Tschitschko et al., 2024), compared to cyanobacterial diazotrophs, the physiological and ecological characteristics of Gamma A are poorly understood, mainly due to the lack of isolated cultures (Turk-Kubo et al., 2023). Still, Gamma A *nifH* is broadly found in open oceans (Cheung et al., 2020; Cornejo-Castillo and Zehr, 2021; Langlois et al., 2015; Shao and Luo, 2022) and occasionally accounts for the majority of the *nifH* transcript pool (Farnelid et al., 2011; Gradoville et al., 2020; Moisander et al., 2014). Since Gamma A *nifH* usually shows higher abundance and transcripts in well-lit waters in oligotrophic subtropical/tropical regions, it has been speculated to prefer warm and low-nutrient conditions (Langlois et al., 2015; Moisander et al., 2014; Turk-Kubo et al., 2023). On the other hand, a recent meta-analysis using the generalised additive model proposed that Gamma A tends to inhabit cold and highly productive regions, such as the subarctic oceans (Shao and Luo, 2022). These inconsistent results emphasise our insufficient understanding of Gamma A distribution and the importance of unexplored controlling factors, such as top-down controls like viral lysis or zooplankton grazing (Shao and Luo, 2022).

Recently, model-based studies have proposed that zooplankton grazing is an important factor that controls the global distribution of diazotrophs (Wang and Luo, 2022; Wang et al., 2019). To date, there have been few quantitative measurements of in situ zooplankton grazing on cyanobacterial diazotrophs. They revealed that the microzooplankton (< 200  $\mu$ m) grazing rate is generally higher on cyanobacterial diazotrophs than on bulk phytoplankton communities in the North Pacific Subtropical Gyre (Turk-Kubo et al., 2018; Wilson et al., 2017), South China Sea (Deng et al., 2023), and Bering Sea (Cheung et al., 2022) and likely controls the abundances of unicellular cyanobacterial diazotrophs (Wilson et al., 2017),

删除: , representing a part of  $\gamma$ -proteobacterial sequences. C

删除: and genomic information other than nitrogenase-related genes...

indicating the potential importance of microzooplankton grazing on NCDs as well. Nevertheless, the microzooplankton grazing rate on NCDs, including that of Gamma A, has never been quantified.

The Kuroshio Current is a western boundary current of the North Pacific that originates in the North Equatorial  
75 Current, enters the East China Sea, flows across the Tokara Strait, and then runs along the Japanese southern coastal area. Although the Kuroshio region is generally characterised by warm and oligotrophic conditions (Chen et al., 2009; Kodama et al., 2014), several nutrient supply processes such as boundary exchange, diapycnal mixing, lateral intrusion, and topographic flow disturbances create biogeochemical variations along the Kuroshio Current (Hasegawa, 2019; Nagai et al., 2019a). Previous studies have reported high nitrogen fixation by numerous cyanobacterial diazotrophs (Chen et al., 2009; Chen et al.,  
80 2019; Cheung et al., 2019; Marumo and Nagasawa, 1976; Shiozaki et al., 2014b; Shiozaki et al., 2015b; Shiozaki et al., 2018a; Wen et al., 2022b). However, these studies were biased toward the upstream region from south Taiwan to southwest Japan, and downstream areas, such as south mainland Japan, were still undersampled (Fig. S1). In southern Japan, seasonal contrasts in nutrient concentrations have been reported (Kodama et al., 2014). Kodama et al. (2021) also found decreased  
85  $\delta^{15}\text{N}$  of particulate organic matter in the nitrate-depleted waters during the summer, inferring active nitrogen fixation in the summer. Additionally, a recent study found a dominance of NCDs with a low abundance of cyanobacterial diazotrophs off the southern coast of Japan in the autumn (Cheung et al., 2019). These results suggest the importance of NCDs, including Gamma A, and a distinct regulation of the diazotroph community in the downstream area compared with that in the upstream area. Recently, the rapid consumption of small phytoplankton by microzooplankton has been suggested as a key factor for the low phytoplankton biomass in the Kuroshio region near Japan (Kanayama et al., 2020; Kobari et al., 2020). Furthermore,  
90 a model-based study predicted that top-down controls, rather than bottom-up controls, regulate the net growth of diazotrophs in a vast area around the Kuroshio region (Wang et al., 2019). These previous studies led us to infer that microzooplankton grazing might play an important role in Gamma A distribution in the Kuroshio region. Therefore, we investigated microzooplankton grazing and growth rates of Gamma A using a combination of the dilution method and quantitative PCR (qPCR) to quantify the microzooplankton grazing pressure on Gamma A at the northern edge of the Kuroshio region, south  
95 of Japan.

## 2 Materials and Methods

### 2.1 Environmental parameters

Our study was conducted during a summer cruise by the R/V *Hakuho-maru* KH-20-09 (10 September to 5 October 2020) and four cruises by R/V *Soyo-maru* (SY2104, Spring [14 April–22, 2021]; SY2109, Summer [3 September–14, 2021];  
100 SY2111, Autumn [17 November–25, 2021]; and SY2201, Winter [12 January–21, 2022]) (Fig. 1, Table 1). The temperature and salinity profiles were measured using an SBE 911 Plus CTD system (Sea-Bird Electronics, Inc., Washington DC, USA). Vertical light attenuation was determined using a PRR-600 (Biospherical Instruments Inc., California, USA) or COMPACT-

删除: and stable isotope ratios of particle organic nitrogen, a proxy for nitrogen fixation,

删除: , in

删除: dicating

删除: seasonal variation in diazotrophy

删除: A

删除: s

删除: understand

LTD (JFE Advantech Co., Ltd., Hyogo, Japan). Water samples for DNA, nutrient, and chlorophyll *a* (Chl *a*) analyses were collected using an acid-cleaned bucket from the surface water and Niskin-X bottles at depths corresponding to 25, 10, and 1 % of the surface light intensity. Nitrate and phosphate concentrations were determined using a QuAAtro autoanalyser (SEAL Analytical, Southampton, UK) or an AACSII autoanalyser (Bran+Luebbe GmbH, Norderstedt, Germany). For Chl *a* analysis, seawater (250 ml) was filtered on 25-mm diameter Whatman GF/F filters (Whatman, Maidstone, UK). Chl *a* was extracted using *N,N*-dimethylformamide and measured using a Turner Design 10 AU fluorometer or Trilogy fluorometer (Turner Designs, California, USA).

Samples (1 L) at the 25 % light depth (13–34 m) for microzooplankton counting were fixed with 2 % Lugol's solution and stored at 4 °C until analysis. After returning to the laboratory, fixed samples were concentrated using reverse filtration with a 10- $\mu$ m mesh. The samples were allowed to settle and condense for at least 24 h. We identified and counted four taxonomic groups of microplankton communities (naked ciliates, tintinids, dinoflagellates, Radiolaria, and copepod nauplii) as potential grazers, using an inverted microscope (ECLIPSE TS100; Nikon Instruments Inc., NY, USA). The size of the cells or individuals was measured, biovolume was computed based on the geometric shape, and carbon content was estimated using conversion equations (Edler, 1979; Mullin, 1969; Putt and Stoecker, 1989; Verity and Lagdon, 1984).

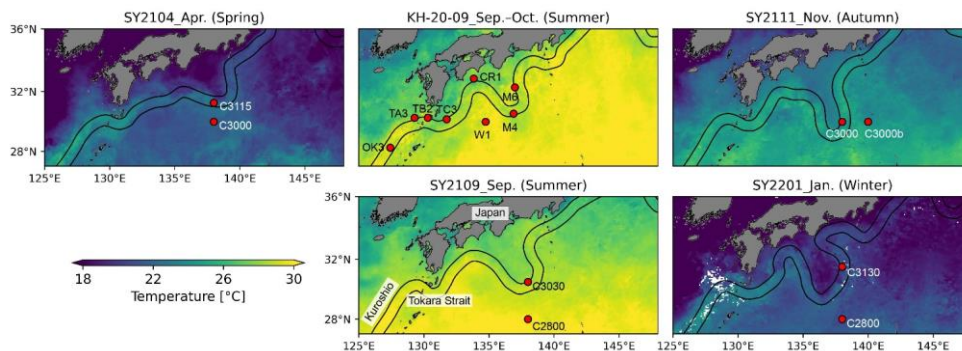


Figure 1. Sampling stations and the paths of the Kuroshio Current during each cruise. Background contours denote sea surface temperature derived from the satellite (MODIS-Aqua) during each cruise. The black lines represent the paths of the Kuroshio Current during the study periods (<http://www1.kaiho.mlit.go.jp/KANKYO/KAIYO/qboc/>).

**Table 1. Summary of environmental variables, Gamma A *nifH* abundance, microzooplankton (MZ) biomass, and parameters derived from the dilution experiments ( $\mu_i$ : nutrient-amended instantaneous rate,  $m$ : mortality rate by microzooplankton grazing,  $\mu_0$ : instantaneous rate without nutrient-amendment,  $k_m$ : nutrient-amended net growth rates) at the 25 % light depth, in which dilution experiments were conducted, off the southern coast of Japan.**

Cruise	Station	Date	25 %	Temp	Nitrate	Phosph	Chl <i>a</i>	Gamma A	MZ	$\mu_i$	$m$	$\mu_0$	$k_m$
			light depth (m)	eratur e (°C)	( $\mu\text{mol}$ $\text{L}^{-1}$ )	ate ( $\mu\text{mol}$ $\text{L}^{-1}$ )	( $\mu\text{g}$ $\text{L}^{-1}$ )	(copies $\text{L}^{-1}$ )	biomass ( $\mu\text{g C L}^{-1}$ )	( $\text{d}^{-1}$ )	( $\text{d}^{-1}$ )	( $\text{d}^{-1}$ )	( $\text{d}^{-1}$ )
SY2104	C3000	17 Apr. 2021	26	21.5	<0.04	<0.02	0.44	$1.80 \times 10^3$	2.92	1.50	1.50	1.83	-0.05
SY2104	C3115	19 Apr. 2021	24	22.7	0.07	<0.02	0.64	$2.60 \times 10^3$	4.23	1.76	1.63	1.73	0.35
SY2109	C2800	5 Sept. 2021	31	29.2	<0.04	<0.02	0.06	$1.91 \times 10^4$	0.84	0.47	0.12	0.65	0.35
SY2109	C3030	7 Sept. 2021	33	27.0	<0.04	<0.02	0.17	$1.31 \times 10^4$	1.67	0.67	0.15	0.67	0.56
KH-20-9	OK3	13 Sept. 2020	16	28.7	<0.04	<0.02	0.09	$1.58 \times 10^3$	2.13	1.35	1.45	1.51	0.12
KH-20-9	TA3	18 Sept. 2020	20	29.1	<0.04	<0.02	0.14	$2.87 \times 10^3$	3.33	1.37	1.61	1.26	0.16
KH-20-9	TB2	21 Sept. 2020	18	28.1	<0.04	<0.02	0.37	$3.00 \times 10^3$	3.36	1.06	0.77	1.13	0.45
KH-20-9	TC3	26 Sept. 2020	20	27.9	<0.04	<0.02	0.22	$3.64 \times 10^3$	3.06	0.93	0.55	1.00	0.37
KH-20-9	W1	28 Sept. 2020	20	28.7	<0.04	<0.02	0.14	$5.41 \times 10^3$	0.88	0.49	0.41	0.76	0.13
KH-20-9	CR1	29 Sept. 2020	20	27.8	<0.04	<0.02	0.18	$3.07 \times 10^3$	0.81	1.48	0.53	1.56	0.94
KH-20-9	M4	1 Oct. 2020	13	27.0	<0.04	<0.02	0.14	$2.44 \times 10^3$	1.16	1.16	0.61	1.24	0.62
KH-20-9	M6	3 Oct. 2020	17	27.8	<0.04	<0.02	0.11	$5.62 \times 10^3$	1.20	0.71	0.67	0.74	0.19
SY2111	C3000b	21 Nov. 2021	29	24.0	<0.04	<0.02	0.27	$5.58 \times 10^3$	2.12	<sup>a</sup>	<sup>a</sup>	<sup>a</sup>	0.21
SY2111	C3000	20 Nov. 2021	26	23.3	0.05	0.05	0.52	$1.00 \times 10^3$	2.41	1.33	0.88	1.34	0.75
SY2201	C2800	18 Jan. 2022	34	20.5	<0.04	0.07	0.58	$2.77 \times 10^3$	0.49	0.37	0.12	0.37	0.29
SY2201	C3130	17 Jan. 2022	23	21.3	<0.04	<0.02	0.44	n.d.	0.49	No	No	No	No

135 <sup>a</sup> Since the slope of regression line was positive, the grazing mortality rate was not determined. <sup>b</sup> Since the Gamma A *nifH* was undetectable at the beginning of the incubation, rates could not be determined. n.d.: Not detected

## 140 2.2 DNA extraction, *nifH* amplicon sequencing, and qPCR analysis

Samples (2.3 L) for DNA analysis were filtered onto 0.22- $\mu\text{m}$  pore size Sterivex-GP filter units (Millipore, Billerica, Massachusetts, USA) and frozen at  $-80^{\circ}\text{C}$  until analysis on land. DNA was extracted using the ChargeSwitch Forensic DNA Purification Kit (Invitrogen, California, USA).

145 To reveal the diazotroph community in the Kuroshio region, *nifH* amplicon sequencing (Zehr and Turner, 2001) were performed on all samples from the 25 % light depth. Both the first and second PCRs were performed under the same conditions:  $94^{\circ}\text{C}$  for 2 min, 30 cycles of  $94^{\circ}\text{C}$  for 30 s,  $52^{\circ}\text{C}$  for 1 min,  $72^{\circ}\text{C}$  for 1 min, and finally  $72^{\circ}\text{C}$  for 7 min. Subsequent analyses of diazotroph communities were performed as previously described (Sato et al., 2021). Briefly, PCR products were sequenced using a MiSeq Reagent Kit v3 (600 cycles; Illumina) and sequencing data were processed with QIIME2 program (ver. 2021.4; Bolyen et al., 2019) to produce sequence variants (SVs) using the Deblur plug-in (Amir et al., 2017). For further analysis, the  
150 sequences were translated into amino acid sequences, and non-*nifH* and frameshift sequences were removed.

Because *nifH* amplicon sequencing revealed that Gamma A was ubiquitous and most abundant in the sequenced *nifH* pool, we estimated its abundance at all light depths (100, 25, 10, and 1 % light depth) using qPCR assays (Moisander et al., 2008) with the MiniOpticon Real-Time PCR Detection System (Bio-Rad, Hercules, California, USA), as described elsewhere (Shiozaki et al., 2015a). The *nifH* standard was obtained by cloning a known *nifH* sequence. All qPCR reactions were  
155 performed in triplicate for each sample. The  $r^2$  values for the standard curves ranged between 0.98 and 1.00, and the PCR efficiencies were between 95.6 % and 99.8 %. No signal was detected in the negative group. Based on the extracted volumes, the detection limit was 75 copies  $\text{L}^{-1}$  seawater.

## 2.3 Estimation of net growth and grazing mortality rates by dilution experiments

Dilution experiments (Landry and Hassett, 1982) with *nifH* qPCR (Cheung et al., 2022; Deng et al., 2023; Turk-Kubo et al., 2018) were conducted to measure the growth and grazing mortality rate of the bulk phytoplankton community and Gamma A at the 25 % light depth. Variations in Chl *a* concentrations and Gamma A *nifH* copies during incubation were used to estimate the growth and grazing mortality rates of the bulk phytoplankton community and Gamma A. It should be noted that the rates of Gamma A were not estimated at St. C3130 in the winter due to an undetectable abundance of Gamma A at the beginning of the incubation.

165 Seawater from the 25 % light depth was prefiltered with 200- $\mu\text{m}$  mesh to remove mesozooplankton and transferred into acid-washed 23-L polycarbonate carboy. Particle-free seawater, prepared by gravity filtration through an acid-washed 0.2- $\mu\text{m}$  filter capsule (Pall Co., Ltd, New York, USA), was mixed with 200- $\mu\text{m}$  prefiltered seawater in acid-washed 2.3-L polycarbonate bottles at four dilution levels: 25, 50, 75, and 100 % with duplicates. These treatment bottles were enriched with 2.0  $\mu\text{mol L}^{-1}$  nitrate ( $\text{NaNO}_3$ ), 0.5  $\mu\text{mol L}^{-1}$  phosphate ( $\text{KH}_2\text{PO}_4$ ), and 0.1  $\mu\text{mol L}^{-1}$  iron ( $\text{FeCl}_3$ ) to avoid nutrient limitation

削除: Carlsbad.

(Landry et al., 2003; Turk-Kubo et al., 2018). Two other bottles filled with 200- $\mu\text{m}$  prefiltered seawater without nutrient enrichment were prepared as controls. The bottles were covered with neutral screens to adjust the light conditions and incubated for 24 h in a water bath with running surface seawater for temperature control. At the beginning and end of the incubation period, all bottles were subsampled for Chl *a* (200 mL) and *nifH* qPCR analysis (2 L). Chl *a* concentration and *nifH* qPCR analysis for Gamma A performed as described above. Here, we assumed that the number of *nifH* copies per cell did not change during the 24 h incubation period.

Net growth rates in each diluted incubation bottle ( $k_i$ ) were estimated as follows:

$$k_i = \frac{\ln N_t - \ln N_0}{t} \quad \text{Eq. (1)}$$

where  $N_t$  and  $N_0$  are the Chl *a* concentrations and Gamma A *nifH* copies at the beginning ( $N_0$ ) and end ( $N_t$ ) of the incubation period ( $t$ : d), respectively.  $k_i$  can be determined with the nutrient-amended instantaneous rate ( $\mu_n$ ) and microzooplankton grazing rate ( $m$ ) using the following equation (Landry and Hassett, 1982):

$$k_i = \mu_n - mD_i \quad \text{Eq. (2)}$$

where  $D_i$  is the dilution level so that the nutrient-amended instantaneous rate ( $\mu_n$ ) and grazing mortality rate ( $m$ ) of each prey can be determined with a linear regression of net growth rate ( $k_i$ ) against dilution level ( $D_i$ ) (Fig. S2). To calculate the in situ instantaneous growth rate ( $\mu_0$ ), we used the sum of net growth rate without nutrient enrichment and the grazing rate (Fig. S2). Differences between  $\mu_n$  and  $\mu_0$  are taken to be indicative of possible nutrient limitation effects (Landry et al., 1998). We also used the nutrient-amended net growth rates of the 100% seawater of Gamma A ( $k_n$ ) to compare current results with previous ones (Fig. S2). Mortality rates were determined only when significant negative regressions ( $p < 0.05$ ) were obtained; otherwise, they were not calculated. Significant regressions were found in all 16 experiments for the bulk phytoplankton community and in 14 out of 16 experiments for Gamma A. It should be noted that, as viral particles are generally smaller than 0.2  $\mu\text{m}$  and there is no serial gradient of viral density in the diluted bottles, the current calculated mortality rate should theoretically be attributed to microzooplankton grazing mortality (Staniewski and Short, 2018).

#### 2.4 Statistical analysis

We used generalized linear mixed models (GLMMs) to assess the relationship between Gamma A abundance and environmental parameters (i.e., temperature, depth, nitrate, phosphate, and Chl *a*) and Gamma A vital rates (i.e.,  $\mu_n$ ,  $\mu_0$ ,  $k_n$ , and  $m$ ), while accounting for sampling non-independence. Since dilution experiments were conducted only at the 25% light depth, we performed two GLMM analyses for Gamma A abundance: one with environmental parameters at all light depths and another with environmental parameters and vital rates at the 25% light depth. Additionally, we conducted a GLMM to examine the relationship between  $m$  of Gamma A and environmental parameters. Before modelling, environmental variables were standardized (mean = 0, standard deviation = 1). Multicollinearity among the environmental variables was assessed

删除:  $\mu$

删除: were

删除:  $\mu$

删除: maximum growth

删除:  $m$

删除:  $\mu_n$

删除: maximum growth rate ( $\mu_{max}$ )

删除:  $\mu$

删除: Net growth rates without nutrient-enrichment ( $\mu_0$ ) were calculated from

删除: enriched

删除: ( $\mu_n$ ), corrected for differences in growth rates between amended and unamended treatments

删除: of 100% seawater

215 using the variance inflation factor (VIF), and variables with a VIF > 3 were excluded from the model. The model was fitted  
using a negative binomial distribution for Gamma A abundance and gamma distribution for *m*, both with log-link function,  
incorporating cruises as a random effect. The Akaike information criterion (AIC) was applied to select explanatory variables,  
and the explanatory variables with the least AIC were candidates for the controlling factors. Marginal  $R^2$  was calculated to  
represent the variation explained by fixed effects, and conditional  $R^2$  to represent the variation explained by both fixed and  
220 random effects. GLMM analyses were conducted using the package “lme4” (Bates et al., 2020) in R software (R Core Team,  
2024)

### 3 Results

#### 3.1 Environmental conditions and microzooplankton community

The sea surface temperature showed a clear temporal variation (Fig. 1 and Fig. S3): higher in the summer (September–  
225 October 2020 and September 2021), lower in the winter (January 2022), and moderate in the autumn and spring (November  
2021). The water temperature at the 25 % light depth, where dilution experiments were conducted, ranged from 20.5 °C to  
29.2 °C (Fig. S3, Table 1) and was higher in the summer (27 °C–29.2 °C) and lower in the winter (20.5 °C and 21.3 °C). The  
nitrate concentration at the 25 % light depth was generally below the detection limit except at St. C3115 during the spring and  
St. 3000 during the autumn, showing 0.07 and 0.05  $\mu\text{mol L}^{-1}$ , respectively (Table 1). Similarly, phosphate was depleted at  
230 most stations, whereas detectable concentrations were observed at St. C3000 in the autumn and St. C2800 in the winter (Table  
1). The Chl *a* concentration at the 25 % light depth was lower in the summer and higher in the spring and winter, ranging  
between 0.09–0.64  $\mu\text{g L}^{-1}$  (Table 1). The highest and lowest concentrations were observed at St. C3115 in the spring and St.  
C2800 in the summer, respectively.

The abundance and biomass of the total microzooplankton community at 25 % light depth ranged 300–3,180 ind.  $\text{L}^{-1}$   
235 and 0.49–4.23  $\text{C } \mu\text{g L}^{-1}$ , respectively (Fig. 2; Table 1). Microzooplankton abundance and biomass were higher in the spring  
and around the Tokara Strait, such as at St. TA3, TB2, and TC3 in the summer, and lower at St. C2800 in the winter and at the  
eastern stations such as St. W1, CR1, and C2800 in the summer. Dinoflagellates and naked ciliates were the two dominant  
taxa, accounting for  $36 \pm 14\%$  and  $34 \pm 17\%$  of total microzooplankton biomass, respectively. Copepod nauplii occasionally  
showed relatively high biomass, with a maximum of 57 % at St. M4 in the summer due to their large body size, although their  
240 proportion of abundance was always below 5 % (Fig. 2).

削除:



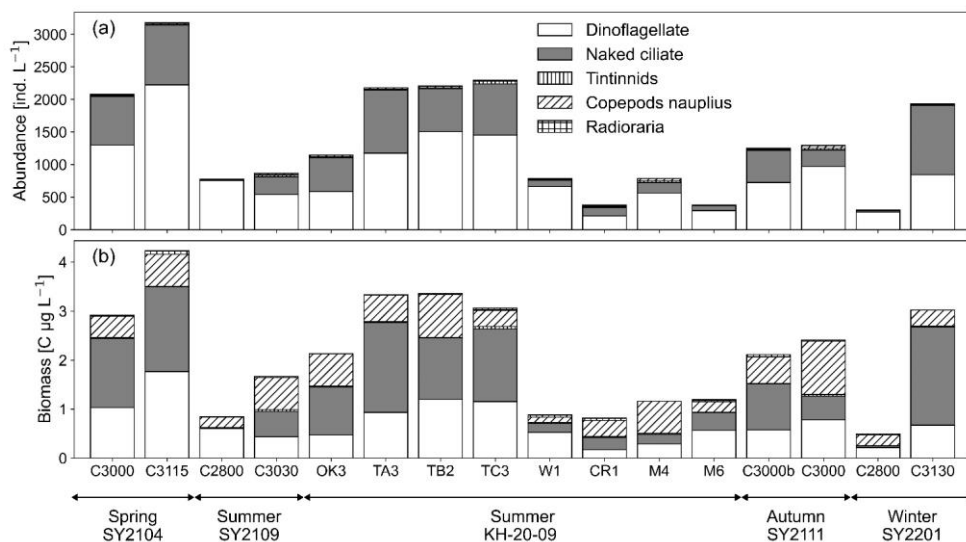


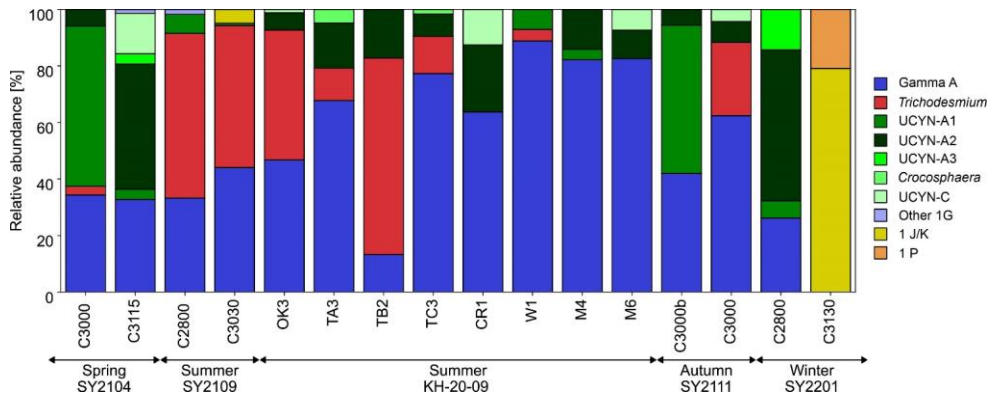
Figure 2. Microzooplankton (a) abundance and (b) biomass for dinoflagellates, naked ciliates, tintinnids, copepods nauplius, and Radiolaria at 25 % light depth at each station around the Kuroshio region

### 3.2 *nifH* gene composition and Gamma A abundance

The *nifH* amplicons from 16 DNA samples at 25 % light depth comprised 70 SVs, of which the 26 most abundant SVs accounted for approximately 97 % of the total sequences at the study stations. Among these major SVs, 21 accounted for 95 % of the total *nifH* sequences, and were affiliated with five well-known diazotrophs: Gamma A (55 %), *Trichodesmium* (18 %), UCYN-A2 (15 %), UCYN-A1 (4.8 %), and UCYN-C (2.9 %) (Fig. S4). The other five SVs included *nifH* Cluster 1B (Cyanobacteria, 2 SVs) and NCDs of *nifH* Clusters 1P (putative  $\delta$ -proteobacteria, 1 SVs) and 1 J/K (putative  $\alpha$ -proteobacteria, 2 SV) (Zehr et al., 2003) (Fig. S4). The most frequently discovered SV, SV001, and 10 other SVs displayed > 97 % similarity at the nucleotide level to Gamma A (Fig. S4). Gamma A was ubiquitous and accounted for  $49 \pm 22$  % of the diazotroph community on average (Fig. 3). At the eastern stations during the summer, such as St. CR1, W1, M4, and M6, Gamma A showed particularly high relative abundances up to 89 % of the total *nifH* sequences (Fig. 3). Cyanobacterial diazotrophs such as *Trichodesmium* and UCYN-A sublineages were occasionally dominant in some samples. UCYN-A1 and UCYN-A2 showed the highest relative abundance, with 57 % of the *nifH* sequences at St. C3000 in the spring and 53 % at St. C2800 in the winter.

260 *Trichodesmium* tended to have higher contributions during the SY2109 cruise and stations west of the Tokara Strait, such as St. OK3 and TB2, during the KH-20-09 cruise in the summer.

The qPCR results also confirmed the extensive occurrence of Gamma A across the study region during the entire season (24 of the 25 stations), ranging from  $1.2 \times 10^2$  to  $1.9 \times 10^4$  copies L<sup>-1</sup> (Fig. S3), with a maximum at 25 % light depth at St. C2800 in the summer. Gamma A tended to be abundant in the summer and was undetectable only at St. C3130 in the winter, whose surface temperature (20.6 °C) was lowest among all the study stations. At the 25 % light depth where the dilution experiments were conducted, Gamma A was detected at all stations except St. C3130 and ranged from  $1.0 \times 10^3$  to  $1.9 \times 10^4$  copies L<sup>-1</sup> (Table. 1).



270 **Figure 3. Diazotroph community composition in the 25 % light depth determined by *nifH* amplicon sequencing in the Kuroshio region.**

### 3.3 Growth and grazing mortality rates of the bulk phytoplankton community and Gamma A

We obtained significant regression lines for all dilution experiments on the bulk phytoplankton community based on changes in Chl *a* ( $p < 0.05$ ; Fig. S2). The grazing mortality rate ( $m$ ; i.e., the slopes of the regression lines in Eq. 2) of the bulk phytoplankton community varied from 0.19–0.82 d<sup>-1</sup> with an average of  $0.45 \pm 0.21$  d<sup>-1</sup> and was the highest rate at St. OK3 in the summer (Fig. 4 (a), Table S1). The nutrient-amended instantaneous growth rate ( $\mu_{\text{ax}}$ ; i.e., the intercepts of the regressions corresponding to  $D_i = 0$  in Eq. 2) of the bulk phytoplankton community ranged from 0.60–1.53 d<sup>-1</sup> with the maximum at the St. C3030 in the summer and the minimum at the St. C3130 in the winter (Fig. 4 (b), Table S1). The instantaneous growth rate without nutrient-amendment ( $\mu_0$ ) was  $0.38 \pm 0.33$  d<sup>-1</sup> (Fig. 5 (a), Table S1).  $\mu_{\text{ax}}$  of bulk phytoplankton community was

- 削除: maximum growth rate
- 削除:  $m$
- 削除:  $\mu_{\text{ax}}$
- 削除: net
- 削除: enrichment
- 削除: and with nutrient-enrichment ( $\mu_{\text{en}}$ ) were
- 削除: –
- 削除: 10
- 削除: 27
- 削除: and  $0.41 \pm 0.23$  d<sup>-1</sup>, respectively (Fig. 5 (a), Table S1).
- 削除:  $e$
- 削除:  $n$

significantly higher than  $\mu_0$  (Paired-sampled  $t$  test;  $p < 0.01$ , Fig. 5 (a)), indicating that net growth rates of bulk phytoplankton community were generally limited by nutrients in the study area except at St. OK3 in the summer and St. 3130 in the winter where nutrient enrichment did not enhance the net growth rates (Fig. S2).

From 15 dilution experiments based on Gamma A *nifH* abundance, we obtained 14 significant negative regression lines ( $p < 0.05$ ; Fig. S5, Table S1). The grazing mortality rate ( $m$ ) of Gamma A varied between 0.12–1.63  $\text{d}^{-1}$  with an average of  $0.73 \pm 0.57 \text{ d}^{-1}$ , and the highest rates were observed at St. C3115 in the spring (Fig. 4 (a), Table 1). The nutrient-amended instantaneous growth rate ( $\mu_n$ ) of Gamma A ranged between 0.37–1.76  $\text{d}^{-1}$  (average:  $1.05 \pm 0.42 \text{ d}^{-1}$ ) with the maximum at the St. SY2104 in the spring and the minimum at the St. C2800 in the winter (Fig. 4 (b), Table 1).  $\mu_n$  and  $m$  had similar trends with a significantly positive correlation with each other ( $r = 0.83$ ,  $p < 0.01$ , Fig. 4 (c)). The in situ instantaneous growth rate ( $\mu_0$ ) was calculated to be 0.37 to 1.83  $\text{d}^{-1}$  (average:  $1.13 \pm 0.45 \text{ d}^{-1}$ ) (Fig. 5 (b), Table 1). In contrast to the bulk phytoplankton community, there is no significant difference between the  $\mu_n$  and  $\mu_0$  of Gamma A (Paired-sampled  $t$  test;  $p > 0.05$ ; Fig. 5 (b)). The  $m$  of Gamma A was significantly higher than that of phytoplankton (Paired-samples  $t$  test,  $p < 0.05$ ), although  $\mu_n$  did not show significant difference between Gamma A and the bulk phytoplankton community. The nutrient-amended net growth rates ( $k_n$ ) of Gamma A were calculated to be  $-0.05$  to  $0.94 \text{ d}^{-1}$  (average:  $0.39 \pm 0.25 \text{ d}^{-1}$ , Table 1).

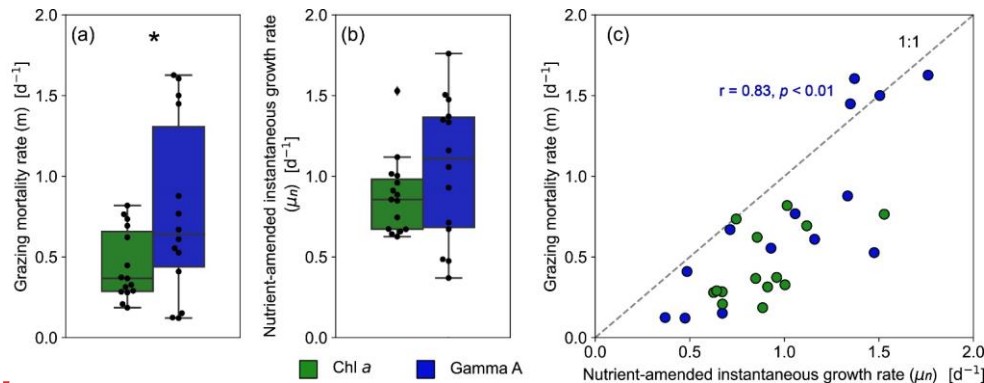


Figure 4. Boxplots comparing the (a) microzooplankton grazing rate ( $m$ ) and (b) nutrient-amended instantaneous growth rate ( $\mu_n$ ) between Gamma A and the bulk phytoplankton community. The asterisk indicates a significant difference between Gamma A and bulk phytoplankton community (Paired-samples  $t$  test;  $p < 0.05$ ). (c) Scatter diagram showing the relationship between  $\mu_n$  and  $m$  of Gamma A and the bulk phytoplankton community. The result of the correlation analysis for Gamma A is shown in blue.

- 删除: S
- 删除: maximum growth rate
- 删除:  $m$
- 删除:  $\mu_n$
- 删除: with
- 删除: S
- 删除:  $m$
- 删除:  $\mu_n$
- 删除: net growth rate without nutrient-enrichment
- 删除: and with nutrient-enrichment ( $\mu_m$ ) were
- 删除: -
- 删除: 4
- 删除: 0
- 删除: 40
- 删除: 27
- 删除: and  $-0.05$  to  $0.94 \text{ d}^{-1}$  (average:  $0.39 \pm 0.25 \text{ d}^{-1}$ ), respectively
- 删除: S
- 删除:  $e$
- 删除:  $n$
- 删除:  $m$
- 删除:  $\mu_n$
- 删除:
- 删除: optimal
- 删除:  $m$
- 删除:  $\mu_n$
- 删除:  $\mu_n$

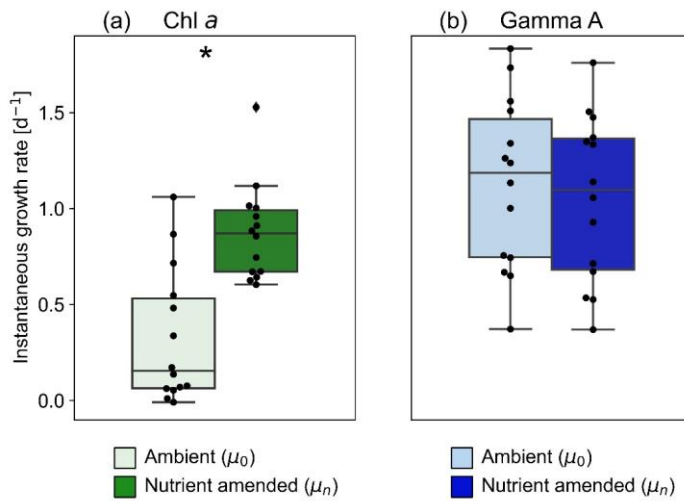
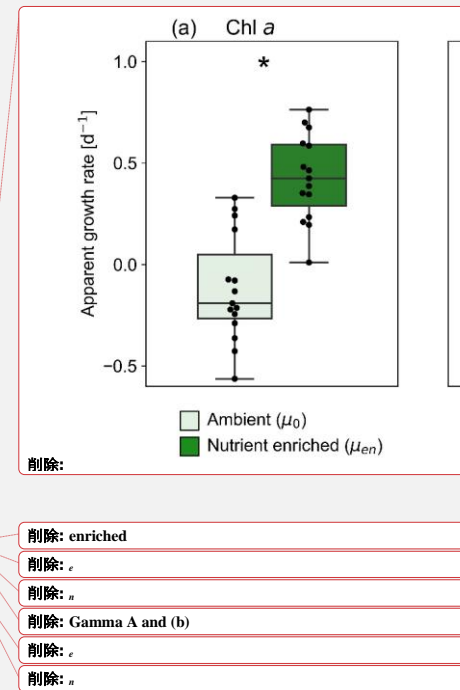


Figure 5. Boxplots comparing the instantaneous growth rates under ambient ( $\mu_0$ ) and nutrient-amended ( $\mu_n$ ) conditions of (a) the bulk phytoplankton community and (b) Gamma A. The asterisk indicates a significant difference between  $\mu_0$  and  $\mu_n$  (Paired-samples  $t$  test;  $p < 0.05$ ).



### 3.4 Environmental variables explaining distribution of Gamma A

In the GLMM approach, temperature and nitrate concentration were selected as explanatory variables for Gamma A abundance across all light depths (Marginal  $R^2 = 0.61$ , Conditional  $R^2 = 0.78$ , Table 2). Temperature had a significant positive effect on Gamma A abundance (coefficient = 1.75,  $p = 2.3 \times 10^{-3}$ ), while nitrate had a significant negative effect (coefficient =  $-2.17$ ,  $p = 5.3 \times 10^{-5}$ ). In the 25% light depth where dilution experiments were conducted,  $m$  and temperature were selected as explanatory variables (Marginal  $R^2 = 0.59$ , Conditional  $R^2 = 0.73$ , Table 2). Among selected parameters,  $m$  had a significant negative relationship with Gamma A abundance (coefficient =  $-0.39$ ,  $p = 6.0 \times 10^{-4}$ ), while temperature showed a positive relationship (coefficient = 0.55,  $p = 8.4 \times 10^{-3}$ ). In addition, GLMM analysis showed that the biomass of the microzooplankton community had a significantly positive effect on the grazing mortality rate of Gamma A (coefficient = 0.36,  $p = 4.7 \times 10^{-3}$ ; Table 2).

**Table 2. The result of the generalized linear mixed model for abundance and grazing mortality rate ( $m$ ) of Gamma A.**

Response variable	Explanatory variables	Coefficient $\pm$ standard error	$t$ -value	$p$ -value	Model $R^2$
Gamma A abundance at all light depth	temperature	$1.75 \pm 0.58$	3.04	$2.3 \times 10^{-3}$	Marginal $R^2 = 0.61$
	nitrate	$-2.17 \pm 0.54$	-4.04	$5.3 \times 10^{-5}$	Conditional $R^2 = 0.78$
Gamma A abundance at the 25% light depth	$m$	$-0.39 \pm 0.11$	-3.43	$6.0 \times 10^{-4}$	Marginal $R^2 = 0.59$
	temperature	$0.55 \pm 0.21$	2.64	$8.4 \times 10^{-3}$	Conditional $R^2 = 0.73$
$m$ of Gamma A	microzooplankton biomass	$0.36 \pm 0.13$	2.83	$4.7 \times 10^{-3}$	Marginal $R^2 = 0.26$ Conditional $R^2 = 0.76$

## 4 Discussion

### 4.1 Dominance of Gamma A in diazotroph communities in the northern edge of the Kuroshio region

Many previous studies have reported abundant cyanobacterial diazotrophs in more upstream areas than in the present study area (Fig. S1), such as the Philippine Sea (Chen et al., 2019; Wen et al., 2022b), southern Taiwan (Chen et al., 2009; Cheung et al., 2019; Shiozaki et al., 2014b; Shiozaki et al., 2018a), the East China Sea (Jiang et al., 2018; Jiang et al., 2023; Chang et al., 2000), and southwestern Japan (Cheung et al., 2019; Shiozaki et al., 2015b; Shiozaki et al., 2018a). In contrast, this study demonstrated that Gamma A is ubiquitous and widely dominant in the diazotroph communities around the northern edge of the Kuroshio Current off the southern coast of Japan (Fig. 3). These results are consistent with a recent high-throughput *nifH* sequencing analysis which found a shift in the diazotroph community from cyanobacteria dominated near Taiwan to NCDs dominated in the south of Japan (Cheung et al., 2019). They also found an eastward decrease in cyanobacterial diazotroph abundance by two to three orders along the Kuroshio Current. This spatial decline in cyanobacterial diazotrophs

删除: Pearson's correlation analysis with Gamma A abundance and environmental variables showed that the abundance of Gamma A had significant correlations with the temperature ( $r = 0.48$ ,  $p < 0.01$ ; Table 2, Fig. S6), nitrate ( $r = -0.37$ ,  $p < 0.01$ ), and phosphate concentrations ( $r = -0.36$ ,  $p < 0.01$ ), but there was no significant correlation with Chl *a* ( $p > 0.05$ ).

删除: Gamma A abundance has significant negative correlations with the  $m$  of Gamma A ( $r = -0.57$ ,  $p < 0.05$ ; Fig. 6 (a), Table 2) and  $\mu_{max}$  of Gamma A ( $r = -0.52$ ,  $p < 0.05$ ; Table 2) at the 25 % light depth in which growth and mortality rates were estimated. I

删除: In addition,

删除: grazing mortality of Gamma A was positively correlated with the ...

删除: Fig. 6 (b).

390 may be attributed to the strong nitrate supply along the Kuroshio path, particularly in Tokara Strait (Nagai et al., 2019b;  
Tsutsumi et al., 2017). The Tokara Strait was reported to have a vertical diffusivity and associated nitrate flux several orders  
of magnitude higher than those in other Kuroshio areas and other open oceans, owing to its steep topographic features (Itoh et  
al., 2021; Kaneko et al., 2013; Kaneko et al., 2021; Tsutsumi et al., 2017). This strong nitrate flux alleviates nitrogen limitation  
on the growth of regional phytoplankton communities (Kobari et al., 2020). Generally, an elevated nitrate supply is considered  
to suppress cyanobacterial diazotroph abundance because they are outcompeted by non-diazotrophic phytoplankton that utilise  
395 resources, such as iron and phosphate, more efficiently (Sato et al., 2022; Ward et al., 2013; Wen et al., 2022b). Consistently,  
this study found a relative decrease of *Trichodesmium* from the western stations (e.g. St. OK3 and TB) to eastern stations (e.g.  
St. CR1 and M4) during a summer cruise KH-20-09 (Fig. 3) and stable abundances of Gamma A in the surface waters between  
 $1.0 \times 10^3$  and  $1.9 \times 10^4$  copies  $L^{-1}$  throughout the study area, except at St. C3130 in the winter (Table 1). Additionally, nitrate  
amendments during the incubation experiments enhanced the growth of the bulk phytoplankton community, a potential  
400 competitor of cyanobacterial diazotrophs, but did not change Gamma A growth (Fig. 5). This suggests that, in contrast to  
cyanobacterial diazotrophs, Gamma A remained abundant and became dominant because of its insensitivity to the turbulent  
nitrate flux along the Kuroshio Current. Still, it should also be noted that the current study only analysed *nifH* DNA, not RNA  
or protein, and that the dominance in the *nifH* DNA pool does not necessarily imply the most active diazotrophs (Shiozaki et  
al., 2017). To confirm the importance of Gamma A as an active diazotroph in the Kuroshio region, future studies should apply  
405 transcriptomic or proteomic approaches.

#### 4.2 Growth characteristics of Gamma A around the Kuroshio region

Little is known about vital rates such as the growth potential of Gamma A mainly due to the lack of established cultures  
(Turk-Kubo et al., 2023 and reference therein). Previous studies reported that nutrient-amended instantaneous growth rates  
( $\mu_{ax}$ ) of unicellular cyanobacterial diazotrophs were higher than or comparable to those of whole phytoplankton communities  
(Cheung et al., 2022; Deng et al., 2023; Turk-Kubo et al., 2018). On the other hand, the growth potential of NCDs, including  
410 Gamma A, has not been examined despite its potential importance on marine nitrogen fixation. This study revealed, for the  
first time, that  $\mu_{ax}$  of Gamma A were between 0.37–1.76  $d^{-1}$ , which were not significantly different from those of whole  
phytoplankton communities (0.60–1.53  $d^{-1}$ ) (Paired-samples *t* test,  $p > 0.05$ , Fig. 4 (b)). Ecosystem models generally presume  
that diazotroph growth is slow because of their need to compensate for the high energetic costs of nitrogen fixation (Dutkiewicz  
et al., 2009; Ward et al., 2013). The current results, however, indicated that not only cyanobacterial diazotrophs but also  
415 Gamma A has growth potential comparable to non-diazotrophic phytoplankton. This highlights the importance of further  
investigations into the growth potential of diazotrophs, including NCDs, to improve global ecosystem models.

There have been only few studies on in situ nutrient-amended net growth rates ( $k_{net}$ ) of Gamma A (Table S2), and the  
observed  $k_{net}$  in the current study (–0.05 to 0.94  $d^{-1}$ ; Table 1) were in line with the previously reported range in the South Pacific  
420 Ocean (up to 0.52; Moisander et al., 2012) and Southwestern Pacific Ocean (–0.91 to 1.07; Turk-Kubo et al., 2015). Although  
significant increases in Gamma A abundance by nutrient or dust additions have been sporadically reported from the

删除: In situ g

删除: in situ  $\mu_{max}$

删除: in situ maximum growth rates (

删除:  $\mu$

删除:  $\mu_{ax}$ )

删除: Fig. 4 (b);

删除: ,

删除: also

删除: enriched

删除:  $\mu_{en}$

删除:  $\mu$

删除: en

删除: Fig. 5 (b)

435 Southwestern Pacific Ocean (Moisander et al., 2012) and eastern North Atlantic Ocean (Langlois et al., 2012), this study found  
no significant response in Gamma A growth due to nitrate, phosphate, and iron enrichment (Paired-samples  $t$  test,  $p > 0.05$ ,  
Fig. 5). Wen et al. (2022a) reported no significant increase in Gamma A abundance with the amendment of iron and/or  
phosphate in the Kuroshio upstream and southeast of Taiwan. This suggests that the growth of Gamma A was not iron- and/or  
phosphate-limited, and other factors, such as temperature and zooplankton grazing, may be more important for the net growth  
440 of Gamma A in the study region. These results inferred that Gamma A may have a distinct ecophysiological trait for iron-  
and/or phosphate-stress from cyanobacterial diazotrophs. For example, as a non-photosynthetic NCD, Gamma A might have  
lower iron requirements than cyanobacterial diazotrophs, which require iron for both photosynthesis and nitrogen fixation. In  
order to confirm their metabolic trait, its genomic contents should be investigated by an omics or isolation approach in the  
future.

#### 445 4.3 Microzooplankton grazing mortality as a controlling factor on Gamma A distribution

Recently, zooplankton grazing on diazotrophs has received attention as an overlooked controlling factor, because  
model-based (Wang et al., 2019; Wang and Luo, 2022) and field studies (Cheung et al., 2022; Deng et al., 2023; Turk-Kubo  
et al., 2018; Wilson et al., 2017) have demonstrated the significance of microzooplankton grazing in the distribution of  
cyanobacterial diazotrophs. However, knowledge of zooplankton grazing on NCDs is still limited to qualitative gut content  
450 analysis (Scavotto et al., 2015), thus, the importance of grazing pressure on NCDs, especially Gamma A, remains unknown.

In this study, we quantified, for the first time, the microzooplankton grazing rate of Gamma A using dilution  
experiments with *nifH* qPCR and found it to be higher than that of the bulk phytoplankton community (Fig. 4 (a)). Furthermore,  
microzooplankton grazing rate of Gamma A had significant negative relationships with Gamma A abundance and positive  
relationships with the biomass of microzooplankton communities (Table 2) which were mainly composed of naked ciliates  
455 and dinoflagellates (Fig. 2). Nitrate and temperature also had negative and positive effects, respectively, on Gamma A  
distribution across all light depths around the Kuroshio (Table 2), consistent with a data compilation of global Gamma A  
abundance (Turk-Kubo et al., 2023). Given that nutrient amendments did not change Gamma A growth during the 24-hour  
incubation, indirect effects, such as resource competition with other organisms under nutrient-replete conditions over longer  
timescales, could reduce regional Gamma A abundance. These suggest that warm and oligotrophic conditions are prerequisites  
460 for Gamma A proliferation and that, under such conditions like the 25% light depth, active microzooplankton grazing likely  
controls Gamma A distribution. High grazing pressure on unicellular cyanobacterial diazotrophs has also been reported in the  
South China Sea (Deng et al., 2023), North Pacific subtropical gyre (Turk-Kubo et al., 2018; Wilson et al., 2017), Bering Sea  
(Cheung et al., 2022), and in laboratory experiments (Deng et al., 2020). Previous studies (Deng et al., 2020; Deng et al., 2023)  
have inferred that this active feeding on diazotrophs could be attributed to their nutritious conditions; unicellular cyanobacterial  
465 diazotrophs tend to have lower C:N ratios than non-diazotrophs, which is indicative of high food quality (John and Davidson,  
2001). Therefore, Gamma A could also be nutritious prey for grazers, resulting in higher grazing pressure in the same manner  
as cyanobacterial diazotrophs. Another possible explanation for the high grazing rate of Gamma A would be its size. Although

删除: ,

删除: :

删除:

删除: distribution

删除: Our study inferred that Gamma A may have a distinct ecological strategy for iron- and/or phosphate-stress from cyanobacterial. ...

删除: ur study

删除: potential

删除: metagenomic

删除: including

删除: Fig. 6,

删除: These results suggest that

删除: possibly

删除: Similarly, h

删除: causing

Gamma A itself may be too small for the prey for microzooplankton, it was found in association with larger size fractions (mainly 3–20  $\mu\text{m}$ ), which has raised speculation of a symbiotic- or particle-bound lifestyle (Benavides et al., 2016; Cornejo-Castillo and Zehr, 2021; Harding, 2021; Tschitschko et al., 2024). This may make the size of Gamma A suitable for the prey for microzooplankton (10–200  $\mu\text{m}$  in this study), considering the optimal size ratio between prey and naked ciliates (1:8), dinoflagellates (1:1), and copepod nauplii (1:18) (Hansen et al., 1994). This explanation is also supported by reports of greater microzooplankton grazing on nano-phytoplankton (2–11  $\mu\text{m}$ ) than other size-fractionated phytoplankton around the Tokara Strait (Kanayama et al., 2020). To validate this explanation, further efforts toward the isolation and in situ visualisation of Gamma A are expected (Harding, 2021). While Gamma A showed the lower grazing mortality rate than its growth rate at some stations, the grazing mortality of Gamma A is generally balanced by the growth rate ( $t$  test,  $p > 0.05$ ; Fig. 4(c)). This contrasted with bulk phytoplankton community, which showed the significantly lower grazing mortality rate than its growth rate ( $t$  test,  $p < 0.01$ ). These results suggest that the nitrogen fixed by Gamma A is rapidly transferred to the food web around the Kuroshio Current with a high turnover rate, possibly sustaining regional biological production. Although the cell-specific nitrogen fixation rate of Gamma A has been challenging, future studies combining our results with such parameters will enable us to discuss the quantitative importance of the nitrogen fixation by Gamma A on marine nitrogen cycle.

## 5 Conclusions

This study quantified the grazing mortality rate of Gamma A around the Kuroshio region for the first time, using dilution experiments and *nifH* qPCR analysis. We found that microzooplankton grazing, as well as nutrient and temperature, played a significant role in the distribution of Gamma A abundance in the study region, reinforcing the importance of top-down controls on diazotroph distribution. Furthermore, we found that the growth and mortality rates of Gamma A was balanced at higher rates than those of the bulk phytoplankton community. Since Gamma A is a major diazotroph in the study region, it may serve as a starting point for the fixed nitrogen derived from nitrogen fixation into the regional food web. Given the widespread presence of Gamma A in subtropical/tropical oligotrophic waters, fixed nitrogen by Gamma A may be broadly introduced into food webs, particularly in warm oligotrophic regions. Further in situ quantification of mortality is required to elucidate the importance of grazing pressure on the global distribution of Gamma A. Additionally, other top-down factors, such as viral lysis, should be explored for further understanding of top-down controls on diazotroph distribution and the associated nitrogen fate in marine ecosystems.

## 510 Author Contribution

TSato and KT designed the experiments. TSato, TY, KH, SS, and TSetou conducted the onboard experiments and water sampling. TSato, TShiozaki, and TK conducted analyses on land. TSato prepared the manuscript draft with contributions from all the co-authors.

删除: It is also noteworthy that t

删除: nearly

删除: Fig. 4(c);

删除: ,

删除: , whereas the

删除: of phytoplankton was significantly lower

删除: Conclutions

删除: successfully

删除: played

删除: Considering the ubiquitous occurrence of Gamma A

删除: can

删除: s on a global scale

删除: .



### **Competing Interests**

The authors declare that they have no conflict of interest.

### **Data Availability Statement**

530 The recovered sequences were deposited in the DNA Data Bank of the Japan Sequence Read Archive under accession  
number DRA019493. The data used in this study were obtained from the UTokyo Repository  
(<http://hdl.handle.net/2261/0002009919>).

### **Acknowledgments**

535 We would like to thank the captain, crew, and participants of R/V Hakuho-maru and R/V *Soyo-maru* for their  
cooperation at sea. We thank H. Saito, H. Morita, and Y. Yoneyama for their kind assistance with water collection and on-  
deck incubation. We also thank Kazuya Takahashi for his kind advice on microscopic observations and R. Ebihara for her  
helpful comments and assistance with MiSeq sequencing. The authors would like to thank Editage ([www.editage.com](http://www.editage.com)) for  
English language editing. This work was supported by JSPS KAKENHI Grant Numbers 19K06198, 20J22451, 20H03059,  
22H03716, 23H02301, 23K26978, and 23KJ1168, the ANRI Fellowship for Young Researchers, and the Fisheries Agency of  
540 Japan through a project titled "Marine Fisheries stock assessment and evaluation for Japanese waters".

## Reference

- Amir, A., McDonald, D., Navas-Molina, J. A., Kopylova, E., Morton, J. T., Zech Xu, Z., Kightley, E. P., Thompson, L. R., Hyde, E. R., Gonzalez, A., and Knight, R.: Deblur rapidly resolves single-nucleotide community sequence patterns, *mSystems*, 2, e00191-00116, 10.1128/mSystems.00191-16, 2017.
- 545 Bates, D., Maechler, M., Bolker, B., Walker, S., Christensen, R. H. B., Singmann, H., Dai, B., Scheipl, F., Grothendieck, G., Green, P., Fox, J., Bauer, A., Krivitsky, P. N., Tanaka, E., and Jagan, M.: lme4: linear mixed-effects models using 'Eigen' and S4, R Package Version, 1–23, 2020.
- Benavides, M., Moisaner, P. H., Daley, M. C., Bode, A., and Aristegui, J.: Longitudinal variability of diazotroph abundances in the subtropical North Atlantic Ocean., *J. Plankton Res.*, 38, 662-672, 10.1093/plankt/fbv121, 2016.
- 550 Bird, C., Martinez, J. M., O'Donnell, A. G., and Wyman, M.: Spatial distribution and transcriptional activity of an uncultured clade of planktonic diazotrophic  $\gamma$ -proteobacteria in the Arabian Sea, *Appl. Environ. Microbiol.*, 71, 2079-2085, 10.1128/AEM.71.4.2079-2085.2005.2005.
- Blais, M., Tremblay, J. É., Jungblut, A. D., Gagnon, J., Martin, J., Thaler, M., and Lovejoy, C.: Nitrogen fixation and identification of potential diazotrophs in the Canadian Arctic, *Glob. Biogeochem. Cycles*, 26, GB3022, 555 10.1029/2011GB004096, 2012.
- Bolyen, E., Rideout, J. R., Dillon, M. R., Bokulich, N. A., Abnet, C. C., Al-Ghalith, G. A., Alexander, H., Alm, E. J., Arumugam, M., Asnicar, F., Bai, Y., Bisanz, J. E., Bittinger, K., Brejnrod, A., Brislawn, C. J., Brown, C. T., Callahan, B. J., Caraballo-Rodríguez, A. M., Chase, J., Cope, E. K., Da Silva, R., Diener, C., Dorrestein, P. C., Douglas, G. M., Durall, D. M., Duvallet, C., Edwardson, C. F., Ernst, M., Estaki, M., Fouquier, J., Gauglitz, J. M., Gibbons, S. M., Gibson, D. L., Gonzalez, 560 A., Gorlick, K., Guo, J., Hillmann, B., Holmes, S., Holste, H., Huttenhower, C., Huttley, G. A., Janssen, S., Jarmusch, A. K., Jiang, L., Kaehler, B. D., Kang, K. B., Keefe, C. R., Keim, P., Kelley, S. T., Knights, D., Koester, I., Kosciolk, T., Kreps, J., Langille, M. G. I., Lee, J., Ley, R., Liu, Y.-X., Loftfield, E., Lozupone, C., Maher, M., Marotz, C., Martin, B. D., McDonald, D., McIver, L. J., Melnik, A. V., Metcalf, J. L., Morgan, S. C., Morton, J. T., Naimey, A. T., Navas-Molina, J. A., Nothias, L. F., Orchanian, S. B., Pearson, T., Peoples, S. L., Petras, D., Preuss, M. L., Pruesse, E., Rasmussen, L. B., Rivers, A., Robeson, M. S., Rosenthal, P., Segata, N., Shaffer, M., Shiffer, A., Sinha, R., Song, S. J., Spear, J. R., Swafford, A. D., Thompson, L. R., Torres, P. J., Trinh, P., Tripathi, A., Turnbaugh, P. J., Ul-Hasan, S., Van Der Hooft, J. J. J., Vargas, F., Vázquez-Baeza, Y., Vogtmann, E., Von Hippel, M., Walters, W., Wan, Y., Wang, M., Warren, J., Weber, K. C., Williamson, C. H. D., Willis, A. D., Xu, Z. Z., Zaneveld, J. R., Zhang, Y., Zhu, Q., Knight, R., and Caporaso, J. G.: Reproducible, interactive, scalable and 565 extensible microbiome data science using QIIME 2, *Nat. Biotechnol.*, 37, 852-857, 10.1038/s41587-019-0209-9, 2019.
- Bombar, D., Paerl, R. W., and Riemann, L.: Marine non-cyanobacterial diazotrophs: moving beyond molecular detection, *Trends Microbiol.*, 24, 916-927, 10.1016/j.tim.2016.07.002, 2016.
- Chang, J., Chiang, K.-P., and Gong, G.-C.: Seasonal variation and cross-shelf distribution of the nitrogen-fixing cyanobacterium, *Trichodesmium*, in southern East China Sea, *Cont. Shelf Res.*, 20, 479-492, 10.1016/s0278-4343(99)00082-5, 2000.
- 575 Chen, M., Lu, Y., Jiao, N., Tian, J., Kao, S. J., and Yao, Z.: Biogeographic drivers of diazotrophs in the western Pacific Ocean, *Limnol. Oceanogr.*, 64, 1403-1421, 10.1002/lno.11123, 2019.
- Chen, Y. L. L., Chen, H. Y., Tuo, S. H., and Ohki, K.: Seasonal dynamics of new production from *Trichodesmium* N<sub>2</sub> fixation and nitrate uptake in the upstream Kuroshio and South China Sea basin., *Limnol. Oceanogr.*, 53, 1705-1721, 10.4319/LO.2008.53.5.1705, 2009.
- 580 Cheung, S., Suzuki, K., Xia, X., and Liu, H.: Transportation of diazotroph community from the upstream to downstream of the Kuroshio, *J. Geophys. Res.: Biogeosci.*, 124, 2680-2693, 10.1029/2018jg004960, 2019.
- Cheung, S., Liu, K., Turk-Kubo, K. A., Nishioka, J., Suzuki, K., Landry, M. R., Zehr, J. P., Leung, S., Deng, L., and Liu, H.: High biomass turnover rates of endosymbiotic nitrogen-fixing cyanobacteria in the western Bering Sea, *Limnol. Oceanogr. Lett.*, 7, 501-509, 10.1002/lol2.10267, 2022.
- 585 Cheung, S., Nitanaï, R., Tsurumoto, C., Endo, H., Nakaoka, S., Cheah, W., Lorda, J. F., Xia, X. M., Liu, H. B., and Suzuki, K.: Physical forcing controls the basin-scale occurrence of nitrogen-fixing organisms in the North Pacific Ocean, *Glob. Biogeochem. Cycles*, 34, e2019GB006452, 10.1029/2019GB006452, 2020.
- Cornejo-Castillo, F. M. and Zehr, J. P.: Intriguing size distribution of the uncultured and globally widespread marine non-cyanobacterial diazotroph Gamma-A, *ISME J.*, 15, 124-128, 10.1038/s41396-020-00765-1, 2021.

590 Delmont, T. O., Pierella Karlusich, J. J., Veseli, I., Fuessel, J., Murat, E. A., Foster, R. A., Bowler, C., Wincker, P., and Pelletier, E.: Heterotrophic bacterial diazotrophs are more abundant than their cyanobacterial counterparts in metagenomes covering most of the sunlit ocean, *ISME J.*, 16, 927-936, 10.1038/s41396-021-01135-1, 2022.

Delmont, T. O., Quince, C., Shaiber, A., Esen, O. C., Lee, S. T. M., Rappe, M. S., MacLellan, S. L., Lucker, S., and Eren, A. M.: Nitrogen-fixing populations of *Planctomycetes* and *Proteobacteria* are abundant in surface ocean metagenomes, *Nat. Microbiol.*, 3, 804-813, 10.1038/s41564-018-0176-9, 2018.

595 Deng, L., Cheung, S., and Liu, H.: Protistal grazers increase grazing on unicellular cyanobacteria diazotroph at night, *Front. Mar. Sci.*, 7, 10.3389/fmars.2020.00135, 2020.

Deng, L., Cheung, S., Xu, Z., Liu, K., and Liu, H.: Microzooplankton grazing exerts a strong top-down control on unicellular cyanobacterial diazotrophs, *J. Geophys. Res.: Biogeosci.*, 128, 10.1029/2023jg007824, 2023.

600 Ding, C., Wu, C., Li, L., Pujari, L., Zhang, G., and Sun, J.: Comparison of diazotrophic composition and distribution in the South China Sea and the Western Pacific Ocean, *Biology*, 10, 10.3390/biology10060555, 2021.

Dutkiewicz, S., Follows, M. J., and Bragg, J. G.: Modeling the coupling of ocean ecology and biogeochemistry, *Glob. Biogeochem. Cycles*, 23, GB4017, 10.1029/2008GB003405, 2009.

Edler, L.: Recommendation on methods of marine biological studies in the Baltic Sea: Phytoplankton and chlorophyll, *The Baltic Marine Biologists Publication*, 5, 1-38, 1979.

605 Farnelid, H., Andersson, A. F., Bertilsson, S., Abu Al-Soud, W., Hansen, L. H., Sorensen, S., Steward, G. F., Hagstrom, A., and Riemann, L.: Nitrogenase gene amplicons from global marine surface waters are dominated by genes of non-cyanobacteria, *PLoS ONE*, 6, e19223, 10.1371/journal.pone.0019223, 2011.

Gradoville, M. R., Farnelid, H., White, A. E., Turk-Kubo, K. A., Stewart, B., Ribalet, F., Ferrón, S., Pinedo-Gonzalez, P., 610 Armbrust, E. V., Karl, D. M., John, S., and Zehr, J. P.: Latitudinal constraints on the abundance and activity of the cyanobacterium UCYN-A and other marine diazotrophs in the North Pacific, *Limnol. Oceanogr.*, 65, 1858-1875, 10.1002/lno.11423, 2020.

Gruber, N. and Galloway, J. N.: An Earth-system perspective of the global nitrogen cycle, *Nature*, 451, 293-296, 10.1038/nature06592, 2008.

615 Halm, H., Lam, P., Ferdelman, T. G., Lavik, G., Dittmar, T., LaRoche, J., D'Hondt, S., and Kuypers, M. M. M.: Heterotrophic organisms dominate nitrogen fixation in the South Pacific Gyre, *ISME J.*, 6, 1238-1249, 10.1038/ismej.2011.182, 2012.

Hansen, B., Bjornsen, P. K., and Hansen, P. J.: The size ratio between planktonic predators and their prey, *Limnol. Oceanogr.*, 39, 395-403, 10.4319/lno.1994.39.2.0395, 1994.

620 Harding, K. J.: Insights into marine unicellular cyanobacterial and noncyanobacterial diazotrophs through single-cell analyses, Ph.D. thesis, University of California Santa Cruz, ark:/13030/m522946f, 2021.

Hasegawa, D.: Island mass effect, in: *Kuroshio Current*, Wiley, 163-174, 10.1002/9781119428428.ch10, 2019.

Itoh, S., Kaneko, H., Kouketsu, S., Okunishi, T., Tsutsumi, E., Ogawa, H., and Yasuda, I.: Vertical eddy diffusivity in the subsurface pycnocline across the Pacific, *J. Oceanogr.*, 77, 185-197, 10.1007/s10872-020-00589-9, 2021.

625 Jiang, Z., Li, H., Zhai, H., Zhou, F., Chen, Q., Chen, J., Zhang, D., and Yan, X.: Seasonal and spatial changes in *Trichodesmium* associated with physicochemical properties in East China Sea and southern Yellow Sea, *J. Geophys. Res.: Biogeosci.*, 123, 509-530, 10.1002/2017jg004275, 2018.

Jiang, Z., Zhu, Y., Sun, Z., Zhai, H., Zhou, F., Yan, X., Zeng, J., Chen, J., and Chen, Q.: Enhancement of summer nitrogen fixation by the Kuroshio intrusion in the East China Sea and southern Yellow Sea, *J. Geophys. Res.: Biogeosci.*, 128, 10.1029/2022jg007287, 2023.

630 John, E. H. and Davidson, K.: Prey selectivity and the influence of prey carbon: Nitrogen ratio on microflagellate grazing, *J. Exp. Mar. Biol. Ecol.*, 260, 93-111, 10.1016/S0022-0981(01)00244-1, 2001.

Kanayama, T., Kobari, T., Suzuki, K., Yoshie, N., Honma, T., Karu, F., and Kume, G.: Impact of microzooplankton grazing on the phytoplankton community in the Kuroshio of the East China sea: A major trophic pathway of the Kuroshio ecosystem, *Deep Sea Res. (I Oceanogr. Res. Pap.)*, 163, 103337, 10.1016/j.dsr.2020.103337, 2020.

635 Kaneko, H., Yasuda, I., Itoh, S., and Ito, S.-I.: Vertical turbulent nitrate flux from direct measurements in the western subarctic and subtropical gyres of the North Pacific, *J. Oceanogr.*, 77, 29-44, 10.1007/s10872-020-00576-0, 2021.

Kaneko, H., Yasuda, I., Komatsu, K., and Itoh, S.: Observations of vertical turbulent nitrate flux across the Kuroshio, *Geophys. Res. Lett.*, 40, 3123-3127, 10.1002/grl.50613, 2013.

- Karl, D., Letelier, R., Tupas, L., Dore, J., Christian, J., and Hebel, D.: The role of nitrogen fixation in biogeochemical cycling in the subtropical North Pacific Ocean, *Nature*, 388, 533-538, 10.1038/41474, 1997.
- 640 Kobari, T., Honma, T., Hasegawa, D., Yoshie, N., Tsutsumi, E., Matsuno, T., Nagai, T., Kanayama, T., Karu, F., Suzuki, K., Tanaka, T., Guo, X., Kume, G., Nishina, A., and Nakamura, H.: Phytoplankton growth and consumption by microzooplankton stimulated by turbulent nitrate flux suggest rapid trophic transfer in the oligotrophic Kuroshio, *Biogeosciences*, 17, 2441-2452, 10.5194/bg-17-2441-2020, 2020.
- 645 Kodama, T., Nishimoto, A., Horii, S., Ito, D., Yamaguchi, T., Hidaka, K., Setou, T., and Ono, T.: Spatial and seasonal variations of stable isotope ratios of particulate organic carbon and nitrogen in the surface water of the Kuroshio, *J. Geophys. Res: Oceans*, 126, 10.1029/2021jc017175, 2021.
- Kodama, T., Shimizu, Y., Ichikawa, T., Hiroe, Y., Kusaka, A., Morita, H., Shimizu, M., and Hidaka, K.: Seasonal and spatial contrast in the surface layer nutrient content around the Kuroshio along 138°E, observed between 2002 and 2013, *J. Oceanogr.*, 70, 489-503, 10.1007/s10872-014-0245-5, 2014.
- 650 Landry, M. R. and Hassett, R. P.: Estimating the grazing impact of marine microzooplankton, *Mar. Biol.*, 67, 283-288, 10.1007/BF00397668, 1982.
- Landry, M. R., Brown, S. L., Campbell, L., Constantinou, J., and Liu, H.: Spatial patterns in phytoplankton growth and microzooplankton grazing in the Arabian Sea during monsoon forcing, *Deep Sea Research Part II: Topical Studies in Oceanography*, 45, 2353-2368, 10.1016/s0967-0645(98)00074-5, 1998.
- 655 Landry, M. R., Brown, S. L., Neveux, J., Dupouy, C., Blanchot, J., Christensen, S., and Bidigare, R. R.: Phytoplankton growth and microzooplankton grazing in high nutrient, low-chlorophyll waters of the equatorial Pacific: community and taxonspecific rate assessments from pigment and flow cytometric analyses, *J. Geophys. Res: Oceans*, 108, 8142, 10.1029/2000jc000744., 2003.
- 660 Langlois, R., Großkopf, T., Mills, M., Takeda, S., and LaRoche, J.: Widespread distribution and expression of Gamma A (UMB), an uncultured, diazotrophic,  $\gamma$ -proteobacterial *nifH* phylotype, *PLoS One*, 10, 10.1371/journal.pone.0128912, 2015.
- Langlois, R., Mills, M., Ridame, C., Croot, P., and LaRoche, J.: Diazotrophic bacteria respond to Saharan dust additions, *Mar. Ecol. Prog. Ser.*, 470, 1-14, 10.3354/meps10109, 2012.
- 665 Luo, Y. W., Doney, S. C., Anderson, L. A., Benavides, M., Berman-Frank, I., Bode, A., Bonnet, S., Boström, K. H., Böttjer, D., Capone, D. G. C., E. J., Chen, Y. L., Church, M. J., Dore, J. E., Falcón, L. I., Fernández, A., Foster, R. A., Furuya, K., Gómez, F., Gundersen, K., Hynes, A. M., Karl, D. M., Kitajima, S., Langlois, R. J., LaRoche, J., Letelier, R. M., Marañón, E., McGillicuddy Jr., D. J. M., P. H., Moore, C. M., Mouriño-Carballido, B. M., M. R. Needoba, J. A., Orcutt, K. M., Poulton, A. J., Rahav, E., Raimbault, P., Rees, A. P., Riemann, L., Shiozaki, T., Subramaniam, A., Tyrrell, T., Turk-Kubo, K. A., Varela, M., Villareal, T. A., Webb, E. A., White, A. E., Wu, J., and Zehr, J. P.: Database of diazotrophs in global ocean: Abundance, biomass and nitrogen fixation rates, *Earth Syst. Sci. Data*, 4, 47-73, 10.5194/essd-4-47-2012, 2012.
- 670 Marumo, R. and Nagasawa, S.: Seasonal variation of the standing crop of a pelagic blue green alga, *Trichodesmium* in the Kuroshio water, *Bull. Plankton Soc. Japan*, 23, 1925, 1976.
- Moisander, P. H., Beinart, R. A., Voss, M., and Zehr, J. P.: Diversity and abundance of diazotrophic microorganisms in the South China Sea during intermonsoon, *ISME J.*, 2, 954-967, 10.1038/ismej.2008.51, 2008.
- 675 Moisander, P. H., Serros, T., Paerl, R. W., Beinart, R. A., and Zehr, J. P.: Gammaproteobacterial diazotrophs and *nifH* gene expression in surface waters of the South Pacific Ocean, *ISME J.*, 8, 1962-1973, 10.1038/ismej.2014.49, 2014.
- Moisander, P. H., Zhang, R., Boyle, E. A., Hewson, I., Montoya, J. P., and Zehr, J. P.: Analogous nutrient limitations in unicellular diazotrophs and *Prochlorococcus* in the South Pacific Ocean, *ISME J.*, 6, 733-744, 10.1038/ismej.2011.152, 2012.
- 680 Mullin, M. M.: Production of zooplankton in the ocean: the present status and problems, *Oceanogr. Mar. Biol. Annu. Rev.*, 7, 293-310, 1969.
- Nagai, T., Clayton, S., and Uchiyama, Y.: Multiscale routes to supply nutrients through the Kuroshio nutrient stream, in: *Kuroshio Current*, Wiley, 105-125, 10.1002/9781119428428.ch6, 2019a.
- Nagai, T., Durán, G. S., Otero, D. A., Mori, Y., Yoshie, N., Ohgi, K., Hasegawa, D., Nishina, A., and Kobari, T.: How the Kuroshio Current delivers nutrients to sunlit layers on the continental shelves with aid of near-inertial waves and turbulence, *Geophys. Res. Lett.*, 46, 6726-6735, 10.1029/2019gl082680, 2019b.
- 685 Putt, M. and Stoecker, D. K.: An experimentally determined carbon : volume ratio for marine "oligotrichous" ciliates from estuarine and coastal waters, *Limnol. Oceanogr.*, 34, 1097-1103, 10.4319/lo.1989.34.6.1097, 1989.
- R Core Team: R: A language and environment for statistical computing [code], <https://www.R-project.org/>, 2024.

- 690 Salazar, G., Paoli, L., Alberti, A., Huerta-Cepas, J., Ruscheweyh, H.-J., Cuenca, M., Field, C. M., Coelho, L. P., Cruaud, C., Engelen, S., Gregory, A. C., Labadie, K., Marec, C., Pelletier, E., Royo-Llonch, M., Roux, S., Sánchez, P., Uehara, H., Zayed, A. A., Zeller, G., Carmichael, M., Dimier, C., Ferland, J., Kandels, S., Picheral, M., Pisarev, S., Poulain, J., Acinas, S. G., Babin, M., Bork, P., Bowler, C., De Vargas, C., Guidi, L., Hingamp, P., Iudicone, D., Karp-Boss, L., Karsenti, E., Ogata, H., Pesant, S., Speich, S., Sullivan, M. B., Wincker, P., Sunagawa, S., Acinas, S. G., Babin, M., Bork, P., Boss, E., Bowler, C., Cochrane, G., De Vargas, C., Follows, M., Gorsky, G., Grimsley, N., Guidi, L., Hingamp, P., Iudicone, D., Jaillon, O., Kandels-Lewis, S., Karp-Boss, L., Karsenti, E., Not, F., Ogata, H., Pesant, S., Poulton, N., Raes, J., Sardet, C., Speich, S., Stemmann, L., Sullivan, M. B., Sunagawa, S., and Wincker, P.: Gene expression changes and community turnover differentially shape the global ocean metatranscriptome, *Cell*, 179, 1068-1083.e1021, 10.1016/j.cell.2019.10.014, 2019.
- 695 Sato, T., Shiozaki, T., Taniuchi, Y., Kasai, H., and Takahashi, K.: Nitrogen fixation and diazotroph community in the subarctic Sea of Japan and Sea of Okhotsk, *J. Geophys. Res.: Oceans*, 126, e2020JC017071, 10.1029/2020JC017071, 2021.
- 700 Sato, T., Shiozaki, T., Hashihama, F., Sato, M., Murara, A., Sasaoka, K., Umeda, S.-i., and Takahashi, K.: Low nitrogen fixation related to shallow nitracline across the eastern Indian Ocean, *J. Geophys. Res.: Biogeosci.*, 127, e2022JG007104., 10.1029/2022JG007104, 2022.
- Scavotto, R. E., Dziallas, C., Bentzon-Tilia, M., Riemann, L., and Moisaner, P. H.: Nitrogen-fixing bacteria associated with copepods in coastal waters of the North Atlantic Ocean, *Environ. Microbiol.*, 17, 3754-3765, 10.1111/1462-2920.12777, 2015.
- 705 Shao, Z. and Luo, Y.-W.: Controlling factors on the global distribution of a representative marine non-cyanobacterial diazotroph phylotype (Gamma A), *Biogeosciences*, 19, 2939-2952, 10.5194/bg-19-2939-2022, 2022.
- Shao, Z., Xu, Y., Wang, H., Luo, W., Wang, L., Huang, Y., Agawin, N. S. R., Ahmed, A., Benavides, M., Bentzon-Tilia, M., Berman-Frank, I., Berthelot, H., Biegala, I. C., Bif, M. B., Bode, A., Bonnet, S., Bronk, D. A., Brown, M. V., Campbell, L., Capone, D. G., Carpenter, E. J., Cassar, N., Chang, B. X., Chappell, D., Chen, Y.-l. L., Church, M. J., Cornejo-Castillo, F. M., Detoni, A. M. S., Doney, S. C., Dupouy, C., Estrada, M., Fernandez, C., Fernández-Castro, B., Fonseca-Batista, D., Foster, R. A., Furuya, K., Garcia, N., Goto, K., Gago, J., Gradoville, M. R., Hamersley, M. R., Henke, B. A., Hörstmann, C., Jayakumar, A., Jiang, Z., Kao, S.-J., Karl, D. M., Kittu, L. R., Knapp, A. N., Kumar, S., LaRoche, J., Liu, H., Liu, J., Lory, C., Löscher, C. R., Marañón, E., Messer, L. F., Mills, M. M., Mohr, W., Moisaner, P. H., Mahaffey, C., Moore, R., Mourriño-Carballido, B., Mulholland, M. R., Nakaoka, S.-i., Needoba, J. A., Raes, E. J., Rahav, E., Ramírez-Cárdenas, T., Reeder, C. F., Riemann, L., Riou, V., Robidart, J. C., Sarma, V. V. S. S., Sato, T., Saxena, H., Selden, C., Seymour, J. R., Shi, D., Shiozaki, T., Singh, A., Sipler, R. E., Sun, J., Suzuki, K., Takahashi, K., Tan, Y., Tang, W., Tremblay, J.-É., Turk-Kubo, K., Wen, Z., White, A. E., Wilson, S. T., Yoshida, T., Zehr, J. P., Zhang, R., Zhang, Y., and Luo, Y.-W.: Global oceanic diazotroph database version 2 and elevated estimate of global oceanic N<sub>2</sub> fixation, *Earth Syst. Sci. Data*, 15, 3673-3709, 10.5194/essd-15-3673-2023, 2023.
- 715 Shiozaki, T., Kondo, Y., Yuasa, D., and Takeda, S.: Distribution of major diazotrophs in the surface water of the Kuroshio from northeastern Taiwan to south of mainland Japan, *J. Plankton Res.*, 40, 407-419, 10.1093/plankt/fby027, 2018a.
- 720 Shiozaki, T., Nagata, T., Ijichi, M., and Furuya, K.: Nitrogen fixation and the diazotroph community in the temperate coastal region of the northwestern North Pacific, *Biogeosciences*, 12, 4751-4764, 10.5194/bg-12-4751-2015, 2015a.
- Shiozaki, T., Ijichi, M., Kodama, T., Takeda, S., and Furuya, K.: Heterotrophic bacteria as major nitrogen fixers in the euphotic zone of the Indian Ocean, *Glob. Biogeochem. Cycles*, 28, 1096-1110, 10.1002/2014GB004886, 2014a.
- 725 Shiozaki, T., Chen, Y. L. L., Lin, Y. H., Taniuchi, Y., Sheu, D. S., Furuya, K., and Chen, H. Y.: Seasonal variations of unicellular diazotroph groups A and B, and *Trichodesmium* in the northern South China Sea and neighboring upstream Kuroshio Current, *Cont. Shelf Res.*, 80, 20-31, 10.1016/j.csr.2014.02.015, 2014b.
- Shiozaki, T., Takeda, S., Itoh, S., Kodama, T., Liu, X., Hashihama, F., and Furuya, K.: Why is *Trichodesmium* abundant in the Kuroshio?, *Biogeosciences*, 12, 6931-6943, 10.5194/bg-12-6931-2015, 2015b.
- 730 Shiozaki, T., Fujiwara, A., Ijichi, M., Harada, N., Nishino, S., Nishi, S., Nagata, T., and Hamasaki, K.: Diazotroph community structure and the role of nitrogen fixation in the nitrogen cycle in the Chukchi Sea (western Arctic Ocean), *Limnol. Oceanogr.*, 63, 2191-2205, 10.1002/lno.10933, 2018b.
- Shiozaki, T., Nishimura, Y., Yoshizawa, S., Takami, H., Hamasaki, K., Fujiwara, A., Nishino, S., and Harada, N.: Distribution and survival strategies of endemic and cosmopolitan diazotrophs in the Arctic Ocean, *ISME J.*, 10.1038/s41396-023-01424-x, 2023.
- 735 Shiozaki, T., Bombar, D., Riemann, L., Hashihama, F., Takeda, S., Yamaguchi, T., Ehama, M., Hamasaki, K., and Furuya, K.: Basin scale variability of active diazotrophs and nitrogen fixation in the North Pacific, from the tropics to the subarctic Bering Sea, *Glob. Biogeochem. Cycles*, 31, 996-1009, 10.1002/2017gb005681, 2017.

- Staniewski, M. A. and Short, S. M.: Methodological review and meta-analysis of dilution assays for estimates of virus- and grazer-mediated phytoplankton mortality, *Limnol. Oceanogr. Methods*, 16, 649-668, 10.1002/lom3.10273, 2018.
- 740 Tschitschko, B., Esti, M., Philippi, M., Kidane, A. T., Littmann, S., Kitzinger, K., Speth, D. R., Li, S., Kraberg, A., Tienken, D., Marchant, H. K., Kartal, B., Milucka, J., Mohr, W., and Kuypers, M. M. M.: Rhizobia–diatom symbiosis fixes missing nitrogen in the ocean, *Nature*, 10.1038/s41586-024-07495-w, 2024.
- 745 Tsutsumi, E., Matsuno, T., Lien, R. C., Nakamura, H., Senjyu, T., and Guo, X.: Turbulent mixing within the Kuroshio in the Tokara Strait, *J. Geophys. Res: Oceans*, 122, 7082-7094, 10.1002/2017jc013049, 2017.
- Turk-Kubo, K. A., Connell, P., Caron, D., Hogan, M. E., Famelid, H. M., and Zehr, J. P.: In situ diazotroph population dynamics under different resource ratios in the North Pacific subtropical gyre, *Front. Microbiol.*, 9, 1616, 10.3389/fmicb.2018.01616, 2018.
- 750 Turk-Kubo, K. A., Frank, I. E., Hogan, M. E., Desnues, A., Bonnet, S., and Zehr, J. P.: Diazotroph community succession during the VAHINE mesocosm experiment (New Caledonia lagoon), *Biogeosciences*, 12, 7435-7452, 10.5194/bg-12-7435-2015, 2015.
- Turk-Kubo, K. A., Gradoville, M. R., Cheung, S., Cornejo-Castillo, F. M., Harding, K. J., Morando, M., Mills, M., and Zehr, J. P.: Non-cyanobacterial diazotrophs: global diversity, distribution, ecophysiology, and activity in marine waters, *FEMS Microbiol. Rev.*, 47, 10.1093/femsre/ruac046, 2023.
- 755 Verity, P. G. and Lagdon, C.: Relationships between lorica volume, carbon, nitrogen, and ATP content of tintinnids in Narragansett Bay, *J. Plankton Res.*, 6, 859-868, 10.1093/plankt/6.5.859, 1984.
- Wang, H. and Luo, Y.-W.: Top-down control on major groups of global marine diazotrophs, *Acta Oceanologica Sinica*, 41, 111-119, 10.1007/s13131-021-1956-2, 2022.
- 760 Wang, W. L., Moore, J. K., Martiny, A. C., and Primeau, F. W.: Convergent estimates of marine nitrogen fixation, *Nature*, 566, 205-211., 10.1038/s41586-019-0911-2, 2019.
- Ward, B. A., Dutkiewicz, S., Moore, C. M., and Follows, M. J.: Iron, phosphorus, and nitrogen supply ratios define the biogeography of nitrogen fixation, *Limnol. Oceanogr.*, 58, 2059-2075, 10.4319/lo.2013.58.6.2059, 2013.
- Wen, Z., Browning, T. J., Dai, R., Wu, W., Li, W., Hu, X., Lin, W., Wang, L., Liu, X., Cao, Z., Hong, H., and Shi, D.: The response of diazotrophs to nutrient amendment in the South China Sea and western North Pacific, *Biogeosciences*, 19, 5237-5250, 10.5194/bg-19-5237-2022, 2022a.
- 765 Wen, Z., Browning, T. J., Cai, Y., Dai, R., Zhang, R., Du, C., Jiang, R., Lin, W., Liu, X., Cao, Z., Hong, H., Dai, M., and Shi, D.: Nutrient regulation of biological nitrogen fixation across the tropical western North Pacific, *Science Advances*, 8, 7564, 10.1126/SCIADV.ABL7564, 2022b.
- Wilson, S. T., Aylward, F. O., Ribalet, F., Barone, B., Casey, J. R., Ferrón, S., Connell, P., Eppley, J. M., Fitzsimmons, J. M., 770 Hayes, C. T., Romano, A. E., Turk-Kubo, K., Vislova, A., Armbrust, E. V., Caron, D. A., Church, M. J., Zehr, J. P., Karl, D. M., and Delong, E. F.: Coordinated regulation of growth, activity and transcription in natural populations of the unicellular nitrogen-fixing cyanobacterium *Crocospaera*, *Nat. Microbiol.*, 2, 17118, 10.1038/nmicrobiol.2017.118, 2017.
- Zehr, J. P.: Nitrogen fixation by marine cyanobacteria, *Trends Microbiol.*, 19, 162-173, 10.1016/j.tim.2010.12.004, 2011.
- Zehr, J. P. and Capone, D. G.: Marine nitrogen fixation, *Springer Nature*, 10.1007/978-3-030-67746-6, 2021.
- 775 Zehr, J. P. and Turner, P. J.: Nitrogen fixation: Nitrogenase genes and gene expression, *Methods Microbiol.*, 30, 271-286, 10.1016/S0580-9517(01)30049-1, 2001.
- Zehr, J. P., Mellon, M. T., and Zani, S.: New nitrogen-fixing microorganisms detected in oligotrophic oceans by amplification of nitrogenase (*nifH*) genes, *Appl. Environ. Microbiol.*, 64, 3444-3450, 10.1128/AEM.64.9.3444-3450.1998, 1998.
- Zehr, J. P., Jenkins, B. D., Short, S. M., and Steward, G. F.: Nitrogenase gene diversity and microbial community structure: a 780 cross-system comparison, *Environ. Microbiol.*, 5, 539-554, 10.1046/j.1462-2920.2003.00451.x, 2003.